PHY 752 Solid State Physics
11-11:50 AM MWF Olin 103

Plan for Lecture 27:

- **Optical properties of semiconductors and insulators (Chap. 7 & 12 in GGGPP)**
  - **Excitons**

13	Wed, 9/23/2015	Chap. 4	Density functional theory	#12
14	Fri, 9/25/2015	Chap. 5	Implementation of density functional theory	#13
15	Mon, 9/28/2015	Chap. 5	Implementation of density functional theory	#14
16	Wed, 9/30/2015	Chap. 5	First principles pseudopotential methods	#15
17	Fri, 10/02/2015	Chap. 6	Example electronic structures	#16
18	Mon, 10/05/2015	Chap. 6	Ionic and covalent crystals	#17
19	Wed, 10/07/2015	Chap. 6	More examples of electronic structures	#18
20	Fri, 10/09/2015	Chap. 1-6	Review	Start exam
	Mon, 10/12/2015		No class	Take-home exam
	Wed, 10/14/2015		No class	Exam due before 10/19/2015
	Fri, 10/16/2015		Fall break -- no class	
21	Mon, 10/19/2015	Chap. 10	X-ray and neutron diffraction	#19
22	Wed, 10/21/2015	Chap. 10	Scattering of particles by crystals	#20
23	Fri, 10/23/2015	Chap. 11	Optical and transport properties of metals	#21
24	Mon, 10/26/2015	Chap. 11	Optical and transport properties of metals	#22
25	Wed, 10/28/2015	Chap. 11	Transport in metals	#23
26	Fri, 10/30/2015	Chap. 12	Optical properties of semiconductors and insulators	
27	Mon, 11/02/2015	Chap. 7 & 12	Excitons	#24
	Wed, 12/02/2015		Student presentations I	
	Fri, 12/04/2015		Student presentations II	
	Mon, 12/07/2015		Begin Take-home final	

Interband transitions

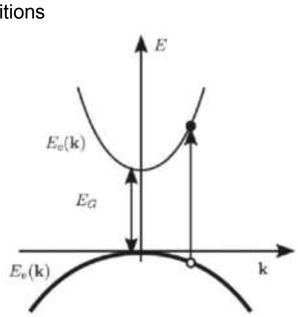

Figure 12.2 Schematic representation of the top valence band and bottom conduction band of a direct gap semiconductor or insulator. Optical transitions are vertical in the energy band diagram. [The valence band has been reported in bold to remind its full occupancy by electrons.]

In general the matrix element $M_{cv}(\mathbf{k})$ is a smooth function of $\mathbf{k}$ and the joint density of states often determines the frequency dependence of the optical properties:

$$J_{cv}(\omega) = \int_{\mathrm{B.Z.}} \frac{d\mathbf{k}}{(2\pi)^3}\delta(E_{c\mathbf{k}} - E_{v\mathbf{k}} - \hbar\omega).$$

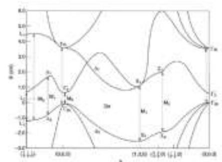

Figure 12.3 Energy bands of germanium along symmetry directions, with the empirical pseudopotential method. The $\mathbf{k}$ wavevector is in units of $2\pi/a$. Relevant direct interband edges are indicated by arrows [With permission from Figs. 1, 2, Phys. Rev. Lett. 9, 94 (1962)].

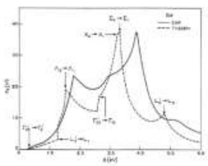

Figure 12.4 Spectral structure of $\varepsilon_2(\omega)$ (solid line) compared with the theoretical results of interband transitions for Ge (dashed line with edges emphasized to account for critical points) [reprinted with permission from D. Brust, J. C. Phillips, and F. Bassani, Phys. Rev. Lett. 9, 94 (1962) and D. Brust, Phys. Rev. 134, A1337 (1964); copyright 1964 by the American Physical Society].

Real spectra and more complete analysis
From Michael Rohlfing and Steven Louie, PRB **62** 4927 (2000)

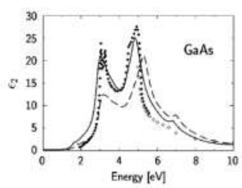

FIG. 6. Calculated optical absorption spectrum of GaAs with (solid lines) and without (dashed lines) electron-hole interaction, using three valence bands, six conduction bands, 500 $\mathbf{k}$ points in the BZ, and an artificial broadening of 0.15 eV. The dots denote experimental data from Ref. 32 (○) and Ref. 33 (●).

Real spectra and more complete analysis
From Michael Rohlfing and Steven Louie, PRB **62** 4927 (2000)

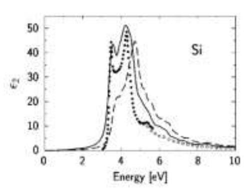

FIG. 8. Calculated optical absorption spectrum of Si with (solid lines) and without (dashed lines) electron-hole interaction, using three valence bands, six conduction bands, 500 $\mathbf{k}$ points in the BZ, and an artificial broadening of 0.15 eV. Experimental data are taken from Ref. 34 (○) and Ref. 35 (●).

Real spectra and more complete analysis
From Michael Rohlfing and Steven Louie, PRB **62** 4927 (2000)

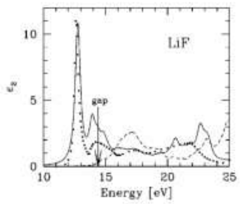

FIG. 9. Calculated optical absorption spectrum of LiF with (solid lines) and without (dashed lines) electron-hole interaction, using three valence bands, six conduction bands, 500 **k** points in the BZ, and an artificial broadening of 0.25 eV. The experimental data (●) are from Ref. 36.

Real spectra and more complete analysis
From Michael Rohlfing and Steven Louie, PRB **62** 4927 (2000)

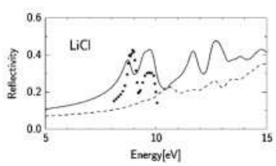

FIG. 10. Calculated reflectivity spectrum of LiCl with (solid lines) and without (dashed lines) electron-hole interaction, using three valence bands, six conduction bands, 500 **k** points in the BZ, and an artificial broadening of 0.25 eV. The experimental data (●) are from Ref. 37.

Simple treatment of exciton effects in a two-band model

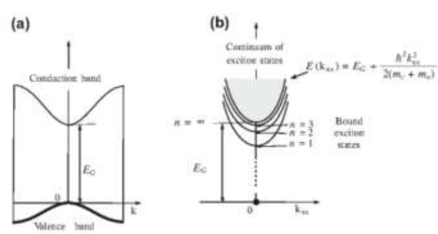

Figure 7.3 (a) Schematic representation of a direct two-band model semiconductor. The lowest conduction band and the highest valence band are shown, assuming band extrema at $\mathbf{k} = 0$ and effective masses m_c and m_v, respectively. The valence band region has been reported in bold to remind its full occupancy by electrons. (b) The electronic ground state of the crystal E_0 (with fully occupied valence band and total wavevector $k_{ex} = 0$) is chosen as zero of energy. The excitonic energy spectrum at $k_{ex} = 0$ is made of discrete levels below E_G and a continuous part above E_G. The curve $E(\mathbf{k}_{ex}) = E_G + \hbar^2 k_{ex}^2/2(m_c + m_v)$ separates the region of discrete exciton levels from the continuum.

Electronic Hamiltonian

$$H_e = \sum_i \frac{\mathbf{p}_i^2}{2m} - \sum_{i,I} \frac{Z_I e^2}{|\mathbf{r}_i - \mathbf{R}_{I0}|} + \frac{1}{2}\sum_{i \neq j} \frac{e^2}{|\mathbf{r}_i - \mathbf{r}_j|},$$

Ground state wavefunction

$$\Psi_0 = \mathcal{A}\{\phi_{v\mathbf{k}_1}\alpha\ \phi_{v\mathbf{k}_1}\beta \ldots \phi_{v\mathbf{k}_N}\alpha\ \phi_{v\mathbf{k}_N}\beta\},$$

Excited state from two-band model summing over wavevectors *k'*

$$\Psi_{ex} = \sum_{\mathbf{k}'} A(\mathbf{k}')\Phi^{(S)}_{c\mathbf{k}'+\mathbf{k}_{ex},v\mathbf{k}'}.$$

Solving Schroedinger equation in this basis:

$$\sum_{\mathbf{k}'} \langle \Phi^{(S)}_{c\mathbf{k}+\mathbf{k}_{ex},v\mathbf{k}} | H_e | \Phi^{(S)}_{c\mathbf{k}'+\mathbf{k}_{ex},v\mathbf{k}'} \rangle A(\mathbf{k}') = EA(\mathbf{k}).$$

Exciton equations -- continued

$$\boxed{\left[E_c(\mathbf{k}+\mathbf{k}_{ex}) - E_v(\mathbf{k}) - E\right] A(\mathbf{k}) + \sum_{\mathbf{k}'} U(\mathbf{k},\mathbf{k}';\mathbf{k}_{ex})A(\mathbf{k}') = 0},$$

where: $U(\mathbf{k},\mathbf{k}';\mathbf{k}_{ex}) = U_1(\mathbf{k},\mathbf{k}';\mathbf{k}_{ex}) + U_2(\mathbf{k},\mathbf{k}';\mathbf{k}_{ex})$

$$U_1(\mathbf{k},\mathbf{k}';\mathbf{k}_{ex}) = -\langle \phi_{c\mathbf{k}+\mathbf{k}_{ex}}\phi_{v\mathbf{k}'} | \frac{e^2}{r_{12}} | \phi_{c\mathbf{k}'+\mathbf{k}_{ex}}\phi_{v\mathbf{k}} \rangle,$$

$$U_2(\mathbf{k},\mathbf{k}';\mathbf{k}_{ex}) = 2\delta_{S,0}\langle \phi_{c\mathbf{k}+\mathbf{k}_{ex}}\phi_{v\mathbf{k}'} | \frac{e^2}{r_{12}} | \phi_{v\mathbf{k}}\phi_{c\mathbf{k}'+\mathbf{k}_{ex}} \rangle.$$

After several steps:

$$U_1(\mathbf{k},\mathbf{k}';\mathbf{k}_{ex}) = -\frac{1}{V}\int e^{-i(\mathbf{k}-\mathbf{k}')\cdot\mathbf{r}}\frac{e^2}{r}\,d\mathbf{r} = -\frac{1}{V}\frac{4\pi e^2}{|\mathbf{k}-\mathbf{k}'|^2} \quad \text{for } \mathbf{k} \approx \mathbf{k}'.$$

Ignoring U_2 for the moment --

$$E_c(\mathbf{k}) = E_G + \frac{\hbar^2 k^2}{2m_c} \quad \text{and} \quad E_v(\mathbf{k}) = -\frac{\hbar^2 k^2}{2m_v} \quad (m_c > 0,\ m_v > 0).$$

$$E_c(\mathbf{k}+\mathbf{k}_{ex}) - E_v(\mathbf{k}) = E_G + \frac{\hbar^2}{2m_c}(\mathbf{k}+\mathbf{k}_{ex})^2 + \frac{\hbar^2 k^2}{2m_v}$$
$$= E_G + \frac{\hbar^2}{2\mu_{ex}}\left(\mathbf{k} + \frac{\mu_{ex}}{m_c}\mathbf{k}_{ex}\right)^2 + \frac{\hbar^2 k_{ex}^2}{2(m_c+m_v)}.$$

Reduced mass: $\dfrac{1}{\mu_{ex}} = \dfrac{1}{m_v} + \dfrac{1}{m_c}$

Equation for k_{ex}=0:

$$\left[E_G + \frac{\hbar^2 k^2}{2\mu_{ex}} - E\right] A(\mathbf{k})$$
$$-\frac{1}{V}\sum_{\mathbf{k}'} \frac{4\pi e^2}{\varepsilon|\mathbf{k}-\mathbf{k}'|^2} A(\mathbf{k}') + \delta_{S,0}\frac{8\pi}{\varepsilon}|\hat{\mathbf{k}}_{ex}\cdot\mathbf{d}_{cv}|^2 \frac{1}{V}\sum_{\mathbf{k}'} A(\mathbf{k}') = 0.$$

Define an envelope function $F(\mathbf{r}) = \dfrac{1}{\sqrt{V}}\sum_{\mathbf{k}'} A(\mathbf{k}')\, e^{i\mathbf{k}'\cdot\mathbf{r}}.$

$$\left[-\frac{\hbar^2\nabla^2}{2\mu_{\mathrm{ex}}} - \frac{e^2}{\varepsilon r} + \delta_{S,0}\frac{8\pi}{\varepsilon}|\widehat{\mathbf{k}}_{\mathrm{ex}} \cdot \mathbf{d}_{\mathrm{cv}}|^2\delta(\mathbf{r})\right] F(\mathbf{r}) = (E - E_G)F(\mathbf{r}).$$

Introduced electron-hole screening

Hydrogen-like eigenstates:

$$E_b^{(\mathrm{ex})} \approx 13.6\,\frac{\mu_{\mathrm{ex}}}{m}\frac{1}{\varepsilon^2} \quad (\text{in eV})$$

$$a_{\mathrm{ex}} = a_B\frac{m}{\mu_{\mathrm{ex}}}\varepsilon$$

Exciton Eigenstates

$$E_n = E_G - \frac{E_{ex}}{n^2}$$

10/30/2015 PHY 752 Fall 2015 -- Lecture 26 13

Some details –

Considered a closed shell system with *N* electrons

$$\Psi_0 = \mathcal{A}\{\phi_1\alpha\,\phi_1\beta \cdots \phi_m\alpha\,\phi_m\beta \cdots \phi_{N/2}\alpha\,\phi_{N/2}\beta\},$$

$$\alpha \Rightarrow \uparrow \qquad \beta \Rightarrow \downarrow$$

We can write the effective Hamiltonian:

$$\left[\frac{\mathbf{p}^2}{2m} + V_{\mathrm{nucl}}(\mathbf{r}) + V_{\mathrm{coul}}(\mathbf{r}) + V_{\mathrm{exch}}\right]\phi_l(\mathbf{r}) = \varepsilon_l\phi_l(\mathbf{r})$$

with

$$V_{\mathrm{coul}}(\mathbf{r}) = 2\sum_j^{N/2}\langle\phi_j(\mathbf{r}')|\frac{e^2}{|\mathbf{r}-\mathbf{r}'|}|\phi_j(\mathbf{r}')\rangle,$$

$$V_{\mathrm{exch}}\phi_l(\mathbf{r}) = -\sum_j^{N/2}\langle\phi_j(\mathbf{r}')|\frac{e^2}{|\mathbf{r}-\mathbf{r}'|}|\phi_l(\mathbf{r}')\rangle\phi_j(\mathbf{r}).$$

10/30/2015 PHY 752 Fall 2015 -- Lecture 26 14

Consider an excitation where an occupied state m is moved to an excited state μ :

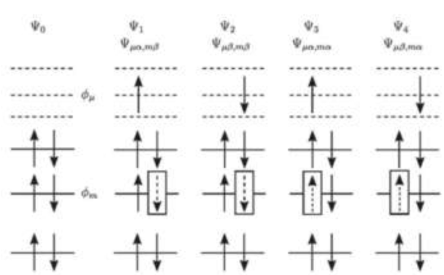

Figure 4.2 Schematic representation of Hartree-Fock occupied and virtual states (here supposed to be discrete) of a closed-shell electronic system. In the four trial excited states Ψ_1, Ψ_2, Ψ_3, and Ψ_4, an electron is promoted from the occupied orbital $\phi_m(\mathbf{r})$ to the virtual orbital $\phi_\mu(\mathbf{r})$.

10/30/2015 PHY 752 Fall 2015 -- Lecture 26 15

Define: $Q_{\mu m} = \langle \phi_\mu(\mathbf{r}_1)\phi_m(\mathbf{r}_2)|\frac{e^2}{r_{12}}|\phi_\mu(\mathbf{r}_1)\phi_m(\mathbf{r}_2)\rangle,$

$J_{\mu m} = \langle \phi_\mu(\mathbf{r}_1)\phi_m(\mathbf{r}_2)|\frac{e^2}{r_{12}}|\phi_m(\mathbf{r}_1)\phi_\mu(\mathbf{r}_2)\rangle.$

$$\langle \Psi_i|H_e|\Psi_j\rangle = E_0 + \varepsilon_\mu - \varepsilon_m + \begin{pmatrix} -Q_{\mu m} & 0 & 0 & 0 \\ 0 & -Q_{\mu m} + J_{\mu m} & J_{\mu m} & 0 \\ 0 & J_{\mu m} & -Q_{\mu m} + J_{\mu m} & 0 \\ 0 & 0 & 0 & -Q_{\mu m} \end{pmatrix} \tag{4.33b}$$

Eigenstates: $E_{\text{triplet}} = E_0 + \varepsilon_\mu - \varepsilon_m - Q_{\mu m}$

$E_{\text{singlet}} = E_0 + \varepsilon_\mu - \varepsilon_m - Q_{\mu m} + 2J_{\mu m}.$

More detailed treatment of U_2 (J) term:

$$U_2(\mathbf{k}, \mathbf{k}'; \mathbf{k}_{\text{ex}}) = 2\delta_{S,0}\langle \phi_{c\mathbf{k}+\mathbf{k}_{\text{ex}}}\phi_{v\mathbf{k}'}|\frac{e^2}{r_{12}}|\phi_{v\mathbf{k}}\phi_{c\mathbf{k}'+\mathbf{k}_{\text{ex}}}\rangle .$$

$$u^*_{c\mathbf{k}+\mathbf{k}_{\text{ex}}}(\mathbf{r}_1)u_{v\mathbf{k}}(\mathbf{r}_1) \approx \frac{1}{V}\langle u_{c\mathbf{k}+\mathbf{k}_{\text{ex}}}|u_{v\mathbf{k}}\rangle .$$

$$\begin{aligned}\langle u_{c\mathbf{k}+\mathbf{k}_{\text{ex}}}|u_{v\mathbf{k}}\rangle &= \langle u_{c\mathbf{k}} + \mathbf{k}_{\text{ex}} \cdot \frac{\partial u_{c\mathbf{k}}}{\partial \mathbf{k}}|u_{v\mathbf{k}}\rangle \\ &= \mathbf{k}_{\text{ex}} \cdot \langle \frac{\partial}{\partial \mathbf{k}} u_{c\mathbf{k}}|u_{v\mathbf{k}}\rangle = i\mathbf{k}_{\text{ex}} \cdot \langle u_{c\mathbf{k}}|\mathbf{r}|u_{v\mathbf{k}}\rangle = i\mathbf{k}_{\text{ex}} \cdot \mathbf{r}_{cv} .\end{aligned}$$

$$\rightarrow \quad U_2(\mathbf{k}, \mathbf{k}'; \mathbf{k}_{\text{ex}}) = \frac{1}{V} 2\delta_{S,0}\frac{4\pi e^2}{k_{\text{ex}}^2}(\mathbf{k}_{\text{ex}} \cdot \mathbf{r}_{cv})(\mathbf{k}_{\text{ex}} \cdot \mathbf{r}^*_{cv})$$

Effective dipole moment: $\mathbf{d}_{cv}/N = e\mathbf{r}_{cv}/N,$

Resulting equation for envelope function:

$$\boxed{\left[-\frac{\hbar^2\nabla^2}{2\mu_{\text{ex}}} - \frac{e^2}{\varepsilon r} + \delta_{S,0}\frac{8\pi}{\varepsilon}|\widehat{\mathbf{k}}_{\text{ex}} \cdot \mathbf{d}_{cv}|^2\delta(\mathbf{r})\right] F(\mathbf{r}) = (E - E_G)F(\mathbf{r})}.$$

Relationships of envelope function:

$$F(\mathbf{r}) = \frac{1}{\sqrt{V}}\sum_{\mathbf{k}'} A(\mathbf{k}')\, e^{i\mathbf{k}'\cdot\mathbf{r}}.$$

$$A(\mathbf{k}) = \frac{1}{\sqrt{V}}\int F(\mathbf{r})e^{-i\mathbf{k}\cdot\mathbf{r}}\,d\mathbf{r}; \quad k^2A(\mathbf{k}) = \frac{1}{\sqrt{V}}\int[-\nabla^2F(\mathbf{r})]e^{-i\mathbf{k}\cdot\mathbf{r}}\,d\mathbf{r};$$

$$-\frac{1}{\sqrt{V}}\sum_{\mathbf{k}'}\frac{4\pi e^2}{\varepsilon|\mathbf{k}-\mathbf{k}'|^2}A(\mathbf{k}') = -\int\frac{e^2}{\varepsilon r}F(\mathbf{r})e^{-i\mathbf{k}\cdot\mathbf{r}}\,d\mathbf{r};$$

$$\frac{1}{\sqrt{V}}\sum_{\mathbf{k}'}A(\mathbf{k}') = \int\delta(\mathbf{r})F(\mathbf{r})e^{-i\mathbf{k}\cdot\mathbf{r}}\,d\mathbf{r};$$

Summary of Wannier exciton analysis

Hydrogen-like eigenstates:

$$E_b^{(\mathrm{ex})} \approx 13.6 \, \frac{\mu_{\mathrm{ex}}}{m} \frac{1}{\varepsilon^2} \quad (\text{in eV})$$

$$a_{\mathrm{ex}} = a_B \frac{m}{\mu_{\mathrm{ex}}} \varepsilon$$

Exciton Eigenstates

$$E_n = E_G - \frac{E_{ex}}{n^2}$$

Wannier analysis is reliable for loosely bound excitons found in semiconductors; for excitons in insulators (such as LiF) Frenkel exciton analysis applies.

Optical absorption due to excitons (Chap. 12)

$$\Psi_{\mathrm{ex}} = \sum_{\mathbf{k}} A(\mathbf{k}) \Psi^{(S=0)}_{c\mathbf{k},v\mathbf{k}} \qquad F(\mathbf{r}) = \frac{1}{\sqrt{V}} \sum_{\mathbf{k}} A(\mathbf{k}) e^{i\mathbf{k}\cdot\mathbf{r}},$$

$$\left[-\frac{\hbar^2 \nabla^2}{2\mu} - \frac{e^2}{\varepsilon r} \right] F(\mathbf{r}) = (E - E_G) F(\mathbf{r}).$$

Transition probability from ground state

$$P_{\Psi_{\mathrm{ex}} \leftarrow \Psi_0} = \frac{2\pi}{\hbar} \left(\frac{eA_0}{mc} \right)^2 2 \left| \sum_{\mathbf{k}} A(\mathbf{k}) \langle \psi_{c\mathbf{k}} | \hat{\mathbf{e}} \cdot \mathbf{p} | \psi_{v\mathbf{k}} \rangle \right|^2 \delta(E_{\mathrm{ex}} - E_0 - \hbar\omega)$$

$$P_{\Psi_{\mathrm{ex}} \leftarrow \Psi_0} = \frac{2\pi}{\hbar} \left(\frac{eA_0}{mc} \right)^2 2 |C_1|^2 V |F(0)|^2 \delta(E_{\mathrm{ex}} - E_0 - \hbar\omega).$$

with $\langle \psi_{c\mathbf{k}} | \hat{\mathbf{e}} \cdot \mathbf{p} | \psi_{v\mathbf{k}} \rangle = C_1$

For spherically symmetric excitons (“first class” transitions)

$$F(0) = 1/\sqrt{\pi a_{\mathrm{ex}}^3 n^3}.$$

$$E_n = E_G - \frac{R_{\mathrm{ex}}}{n^2} \; (n = 1, 2, 3, \ldots) \quad \text{and intensities} \quad I_n \div \frac{1}{\pi a_{\mathrm{ex}}^3 n^3}.$$

For *p*-like excitons (“second class” transitions)

$$\langle \psi_{c\mathbf{k}} | \mathbf{p} | \psi_{v\mathbf{k}} \rangle = C_2 \mathbf{k};$$

$$P_{\Psi_{\mathrm{ex}} \leftarrow \Psi_0} = \frac{2\pi}{\hbar} \left(\frac{eA_0}{mc} \right)^2 2 |C_2|^2 V |\hat{\mathbf{e}} \cdot \nabla F(\mathbf{r})_{\mathbf{r}=0}|^2 \delta(E_{\mathrm{ex}} - E_0 - \hbar\omega).$$

$$E_n = E_G - \frac{R_{\mathrm{ex}}}{n^2} \quad (n = 2, 3, 4, \ldots) \quad \text{and intensities} \quad I_n \div \frac{n^2 - 1}{\pi \, a_{\mathrm{ex}}^5 n^5}.$$

Example of Cu_2O:

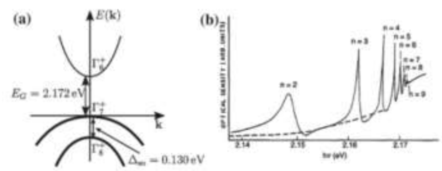

Figure 12.11 (a) Schematic band structure of Cu_2O showing the conduction band, and the valence bands, split by spin-orbit interaction. (b) Absorption spectrum of the yellow exciton series in Cu_2O at 1.8 K [from K. Shindo, T. Goto and T. Anzai, J. Phys. Soc. Japan 36, 753 (1974)]. Since the band-to-band transition is dipole forbidden at the symmetry point $\mathbf{k} = 0$, the exciton series begins with the line $n = 2$.